SURFACE AND INTERFACE ANALYSIS
Surf. Interface Anal. 2006; **38**: 378–382
Published online in Wiley InterScience
(www.interscience.wiley.com). DOI: 10.1002/sia.2152

Surface and Interface Analysis

Metastable impact electron emission microscopy: principles and applications

G. Lilienkamp[1]* and Y. Suchorski[2]

[1] Institut für Physik und Physikalische Technologien, Technische Universität Clausthal, Leibnizstr 4, D-38678 Clausthal-Zellerfeld, Germany
[2] Chemisches Institut, Otto-von-Guericke-Universität Magdeburg, Universitätsplatz 2, D-39106 Magdeburg, Germany

Received 27 June 2005; Revised 14 October 2005; Accepted 19 October 2005

Metastable impact electron emission microscopy (MIEEM) provides a mesoscopic visualization of surfaces by electrons emitted owing to metastable He^*-atom (2^3S) impacts and a spectroscopic contrast by an imaging energy filter. Since the metastable He^* atoms excite the outermost surface electrons solely, a high surface sensitivity is achieved. The MIEEM imaging mode was realized by the combination of the He^* source with the spectroscopic low energy electron microscope (SpecLEEM), thus allowing a reliable tracing of spatiotemporal surface processes within the field of view of *ca* 50 μm diameter. A few examples of MIEEM-applications are presented: a study of the chemical composition of insulating islands appearing on lanthanum-doped $SrTiO_3$(100) surfaces as well as the first successful employment of MIEEM for the *in situ* imaging of surface reactions. Copyright © 2006 John Wiley & Sons, Ltd.

KEYWORDS: MIES; MIEEM; $SrTiO_3$; catalytic surface reaction; alkali metals; coadsorption

INTRODUCTION

Imaging electron spectroscopy has made remarkable progress during the last 10 years. This has been achieved mainly by the introduction of high brightness synchrotron radiation sources and by the refinement of the low energy electron, the photoelectron emission microscope[1] and scanning photoemission microscopes (SPEM).[2] However, the limited access to synchrotron radiation stimulates the efforts to extend the number of possible excitation sources. Independently, it is of interest to explore contrast mechanisms in spectromicroscopy that could provide additional information compared to established microscopes.

Metastable impact electron emission microscopy (MIEEM) based on the utilization of electrons emitted in thermal collisions of excited He^* atoms fulfills, in principle, the requirements for a chemically-resolved imaging of surfaces. In this contribution, we present an overview of our recent work performed in the MIEEM-mode of the spectroscopic low energy electron microscope (SpecLEEM) combined with an intensive He^* source.

BASICS AND EXPERIMENTAL

Metastable impact electron spectroscopy (MIES) or metastable atom electron spectroscopy (MAES) has been used as a surface sensitive technique since the early work of Hagstrum.[3] In MIES, an excited noble gas atom in a metastable state (e.g. He^* in the 2^3 S state with $E^* = 19.82$ eV), which cannot decay via dipole transition, transfers its energy to a target during collision. The main deexcitation processes are resonance ionization (RI) followed by Auger neutralization (AN) and Auger deexcitation (AD). If there is no possibility for RI (e.g. at low work function materials and for many oxides), the major process is AD with a transition from a valence electron to the ground level hole of the metastable atom and emission of the excited noble gas electron. A detailed survey of MIES can be found in the review articles by Morgner[4] and Harada *et al*.[5]

In comparison to UV- and X-ray excited electron spectroscopy, the benefits of MIES are the exclusive surface sensitivity – only electronic states at the outermost surface give a contribution to the MIES signal – and the vanishing sample destruction since the kinetic energy of metastable atoms is in the thermal range. Possible applications of a MIES-based microscopy would be the study of the interaction of adsorbed species, e.g. in catalytic processes, examination of radiation-sensitive materials like polymer films, phase transitions at surfaces especially with changes in the molecular orientation of adsorbed species, and some special questions in the modification of surfaces such as segregation and termination of surfaces. Thus, it seems worthwhile to prove the potential of an emission microscopy with excitation by metastable atoms, which we call MIEEM.

The first question to be answered is whether the flux density of emitted electrons is sufficient for the imaging of a field of view of about 50 μm or smaller, with a spatial resolution at least in the 100-nm range and with acquisition time of a few seconds. Harada *et al*.[6,7] have already shown that MIEEM is working in principle but where are the limits? To realize the MIEEM as an effectively working device, an

*Correspondence to: G. Lilienkamp, Institut für Physik und Physikalische Technologien, Technische Universität Clausthal, Leibnizstr 4, D-38678 Clausthal-Zellerfeld, Germany.
E-mail: Gerhard.lilienkamp@tu-clausthal.de
Contract/grant sponsor: Deutsche Forschungsgemeinschaft.

intensive He^* source is needed. The principle of the He^* source developed in Clausthal has been described in detail previously.[8] Metastable He^* ($2^3S/2^1S$) ($E^* = 19.8/20.6$ eV) atoms with thermal kinetic energies and HeI photons ($E^* = 21.2$ eV) are produced in a cold-cathode gas discharge. In order to increase the He^* beam intensity, a second discharge is ignited between the source anode and skimmer.[9] Under the chosen working conditions, the spectra are only determined by $He^*(2^3S)$. By using a hexapole magnet, the $He^*(2^3S)$ atoms with a particular spin orientation can be focused to improve the flux density, which is in the range of about 10^{10} photon/mm^2∗s before focusing. This value seems to be quite small in comparison to modern synchrotron radiation sources where $n_{photon} = 10^{16}$ photons/mm^2∗s are achievable. But since the electron yield in MIES is of the order of 1, the cross section may compensate for, at least partially, the difference in the incoming flux density.

A detailed description of the LEEM microscope with an energy filter (SpecLEEM), which is the basis of our MIEEM is given in.[1,10] Emitted electrons are accelerated by a homogeneous field between the sample and the first electrode of the combined electrostatic/magnetic objective lens to a kinetic energy of 18 keV. The following lens system transfers the diffraction pattern from the back focal plane of the objective lens to the contrast aperture and further to the entrance of the electrostatic 180° electrostatic energy filter. The 'detected' energy is set by the sample potential (starting voltage = (STV)). An energy resolution of greater than 400 meV can be achieved by decelerating the electrons in front of the energy filter. Behind the filter, the electrons are accelerated again to 18 keV, pass the energy selection slit and the final image is projected onto a chevron-type channel plate array used as image amplifier. Astigmatism introduced by elements with curved axes such as the beam splitter and the energy filter can be reduced by sets of quadrupoles.

APPLICATIONS

Two examples of the MIEEM-application are presented: a study of the chemical composition of insulating islands appearing on lanthanum-doped $SrTiO_3$(100) surfaces as well as the first successful employment of MIEEM for probing the spatial distribution of adsorbates on metal surfaces and for the *in situ* imaging of surface reactions.

Segregation at $SrTiO_3$(100) surfaces

The first of our test systems was a 5% La-doped $SrTiO_3$(100) sample after 120 h at 1300 °C in air cleaned by a short flash to 973 K in UHV. $SrTiO_3$ is a candidate for an alternative oxygen sensor and the heating process was chosen to inspect the degradation under employment conditions. The working principle of a $SrTiO_3$ oxygen sensor is based on changes of the electrical conductivity by creation and annihilation of oxygen vacancies depending on the oxygen partial pressure. In Fig. 1, a PEEM image and three energy filtered MIEEM images show segregation of islands with a height of the order of 100 nm (AFM results). These islands consist of SrO (SAM results[11]) and degrade the function of the sensor due to the low conductivity for oxygen. At least three different sectors can be distinguished by MIEEM: (i) a big segregated island in the center and a thin needle-like island pointing upwards, (ii) a flat surrounding at more than 2 μm distance from the islands and (iii) a small rim enclosing the islands. Regions of interest [ROIs, 2×2 μm^2 for the sectors (i) and (ii) and 1×1 μm^2 for the sector (iii)] indicated in Fig. 1 (upper part) were placed and corresponding spectra were evaluated from the MIEEM series (Fig. 1, lower part). A comparison with the spectra for a reference sample shows that the surface regions a few μm away from the islands have $SrTiO_3$ composition. The spectra from the islands themselves are much wider than the spectra from the reference SrO sample. The width of the spectrum can be explained by a SrO_2-like structure, comparable to MgO_2 where valence band peak positions are marked in Fig. 1.[11] Thus, we assume an island termination with an electronic structure comparable to SrO_2. The 2-μm wide rim around the islands that could not be detected by STM, SAM or AFM exhibits a higher density closer to the Fermi level and herewith a more semiconducting behavior. Due to the formation of the islands a loss of Sr in the surrounding rim occurs. Thus, the phase in this region should have a higher Ti concentration than $SrTiO_3$, presumably close to that in TiO_2 or in Ti_2O_3.[11]

Catalytic H_2 oxidation on Rh(110)

The nonlinear kinetics in surface reaction systems often results in inhomogeneous distributions of adsorbed species that can be visualized *in situ* by various microscopic imaging techniques such as PEEM, LEEM[12] STM, field emission microscopy (FEM), and field ion microscopy (FIM),[13,14] respectively. Unfortunately, the absence of the chemical sensitivity considerably limits the possibilities of these methods since the intensity distributions in the obtained images cannot always be unambiguously interpreted without additional spectroscopic information. This principal shortcoming becomes especially perceivable in the case where more than two types of species are participating in the reaction, i.e. in the case of a promoted catalytic reaction, where e.g. an alkali metal is used as an additive. The diffusion of such additives that are mobile at the reaction conditions adds additional complexity to the observed pattern formation because of the dynamical self-organization effects in the diffusion zone.[15,16] Such self-organization effects during the potassium-doped catalytic $O_2 + H_2$ reaction were recently observed by PEEM and SPEM and explained using the spectroscopic ability of SPEM.[17,18] We have taken the same reaction system ($O_2 + H_2$/K/Rh(110)) as a test of the MIEEM abilities to trace *in situ* the dynamic surface processes.[19]

The clean Rh(110) surface was first imaged with MIEEM and the corresponding MIES spectra were obtained by integrating the intensity within various ROIs (*ca* 2×2 μm^2) in a series of images obtained with different electron energies. The same procedure was repeated for the oxidized and hydrogen-reduced surface, revealing differences in the emission from hydrogen-reduced and oxygen-covered surfaces that are sufficient for a clear contrast.[19]

In the case of the K-precovered surface, the interpretation of the images becomes difficult, since the local emission depends essentially on the local K-coverage, which is

DOI: 10.1002/sia

Surface and Interface Analysis

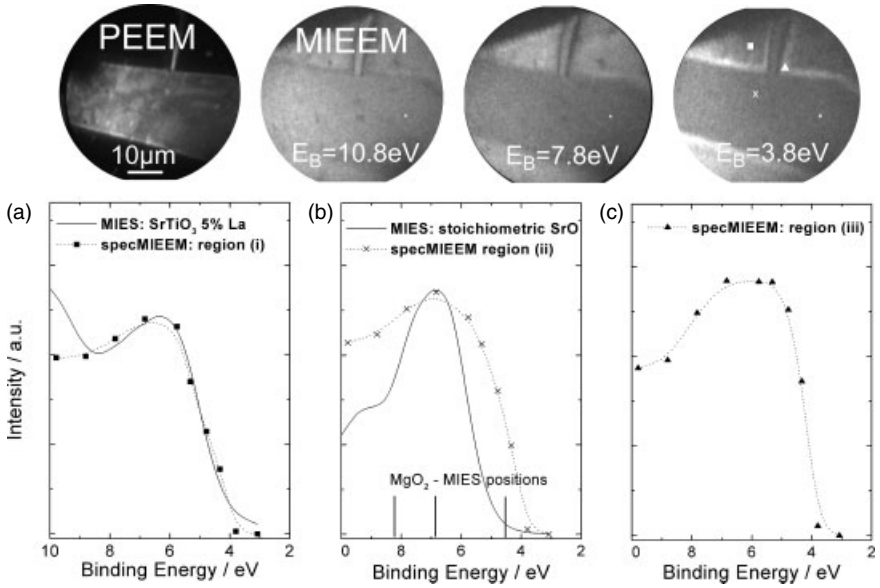

Figure 1. PEEM and MIEEM images of a $SrTiO_3$ (100) surface after heating in air at 1300 °C for 120 h. Three different ROI-positions are marked: region (a) square symbol, region (b) cross symbol, and region (c) triangle symbol. Dotted lines with analogous symbols display the corresponding MIEEM spectra integrated at ROIs indicated above. For the region (b), the calculated positions for MIES features from MgO_2 are marked on the energy axis. Based on Ref. 11.

not necessarily homogeneous during the reaction process. Figure 2 displays the emission spectra for the reduced and oxidized K-precovered surface.[19] The differences in the spectra allow for the sufficient contrast at different energies, whereas a contrast reversal is expected when changing from the lower energy edge to higher kinetic energies. Similarly, as in the case of the K-free surface, the spectra provide a reliable attribution of the different species in the MIEEM pictures. A contrast reversal is in fact observed proving thus the picture interpretation (compare images taken at STV = 14 and 3 V correspondingly).

The achieved chemical sensitivity allowed us to reproduce the main result of the SPEM study,[17] namely, to observe the self organization of the potassium layer via surface diffusion of potassium in the presence of two different spatially separated surface phases (oxidized and reduced Rh surface). Evidence of the potassium redistribution can be found in the images in Fig. 3. Already, the PEEM image with a dark region in the middle of the oxygen-covered area, suggests potassium depletion in the central region and a K-enrichment in the front region. The verification of this suggestion is given by the corresponding MIEEM image taken at STV = 4 V: the dark spot in the PEEM image appears as a bright spot in MIEEM covering the same part of the oxidized surface, as can be concluded from the image-brightness profiles across the oxidized area.[19]

The redistribution of potassium during the ongoing hydrogen oxidation can be explained in terms of the chemically-assisted uphill diffusion: as was noted earlier in the SPEM study,[17] the energetically more favorable adsorption sites of K in the oxygen coadsorbate phase lead to K-redistribution due to the chemical potential gradient. We would like to emphasize here that the self-organization effects caused by the uphill diffusion of electropositive adsorbates have been already observed

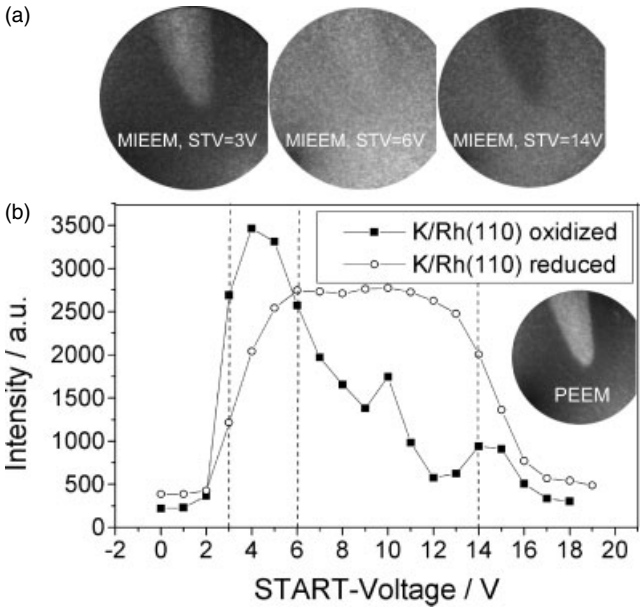

Figure 2. An *in situ* visualization of the H_2 oxidation reaction on the K-precovered Rh(110) surface ($\Theta_K = 0.17$).
(a): MIEEM-images at T = 570 K, $p_{O_2} = 2 \times 10^{-7}$ mbar, $p_{H_2} = 1.2 \times 10^{-7}$ mbar; STV = 3 V, STV = 6 V (no contrast is expected at this voltage, see spectra below); and STV = 14 V (note the reverse of the contrast with respect to STV = 3 V). The inset shows the corresponding PEEM image. (b) MIEEM spectra from the oxidized and hydrogen-reduced Rh(110) surface obtained by He* (2^3 S) excitation. Based on Ref. 19.

in two-dimensional, first-order phase transitions under reaction-free conditions.[20]

Similar to the SPEM experiments,[17] our MIEEM observations[19] show the slowing down of the propagation of the reaction fronts, an effect obviously related to the increased

DOI: 10.1002/sia

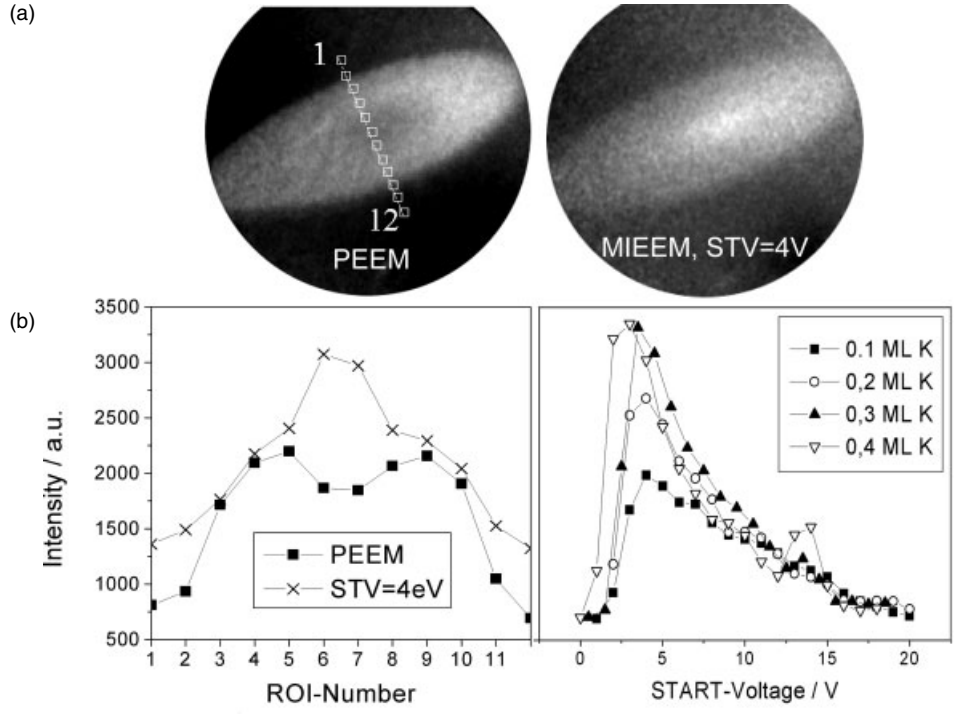

Figure 3. Reaction-induced redistribution of the coadsorbed potassium in the H_2 oxidation on the K-precovered Rh(110) surface ($\Theta_K = 0.2$). (a) PEEM image of the ongoing reaction at T = 570 K, $p_{O_2} = 2 \times 10^{-7}$ mbar, $p_{H_2} = 1.2 \times 10^{-7}$ mbar. The dark region in the middle of the oxygen-covered surface points to the depletion of the K-layer; MIEEM image (STV = 4 V). The corresponding K-depleted region exhibits a higher electron emission. (b) Intensity profiles of the PEEM and MIEEM images evaluated along the line of ROIs shown in the PEEM image; MIEEM spectra from the oxygen-covered and hydrogen-reduced K-precovered Rh(110) surface obtained at different potassium coverages. The differences in the emission at lower STVs are sufficient to register the changes in the K-coverage during the reaction. Based on Ref. 19.

concentration of alkali in the front region. Recently, a steep decrease in the reaction rate in the CO oxidation on different Pt surfaces was observed at increasing coverage of the electropositive coadsorbates such as alkali (Li) or alkaline earth (Dy) that function rather as poisons than as promoters in the H_2- or CO-oxidation reactions.[15,17,21,22] When the reaction rate approaches zero, a natural slowing down of the propagation of the reaction front can be expected, especially when one considers the low mobility of the dissociatively-adsorbed oxygen on the alkali-precovered surface.

SUMMARY AND OUTLOOK

The most useful advantage of the MIEEM is the possibility to obtain additional information from a direct comparison of the images obtained by various imaging techniques such as LEEM and PEEM applied to the same surface region. The exclusive surface sensitivity of the MIES process, which serves as a basis for MIEEM, allows extracting data originating solely from the outermost surface layer. Many situations can be imagined where the structures could be visualized that are not visible with alternative techniques: e.g. different substituent positions at a benzene ring of organic molecules or even different molecular orientations at the surface might lead to remarkable contrasts. A comparison of 2- and 4-chlorobenzylmercaptan molecules on an Au substrate, which differ solely by the position of the Cl but produce significantly distinguishing MIES spectra[23], gives an impression of the potential of MIEEM. Thus, especially MIEEM imaging of domains of spatially inhomogeneously oriented molecules and of phase transitions with orientational changes seems to be very promising.

Acknowledgements

Support by the Deutsche Forschungsgemeinschaft is gratefully acknowledged.

REFERENCES

1. Schmidt Th, Heun S, Slezak J, Diaz J, Prince K, Lilienkamp G, Bauer E. *Surf. Rev. Lett.* 1998; **5**: 1287.
2. Günther S, Kaulich B, Gregoratti L, Kiskinova M. *Prog. Surf. Sci.* 2002; **70**: 187.
3. Hagstrum HD. *Phys. Rev.* 1954; **96**: 336.
4. Morgner H. *Adv. Atom Mol. Opt. Phy.* 2000; **42**: 387.
5. Harada Y, Masuda S, Ozaki H. *Chem. Rev.* 1997; **97**: 1897.
6. Harada Y, Yamamoto S, Aoki M, Masuda S, Ichinokawa T, Kato M, Sakai Y. *Nature* 1994; **372**: 657.
7. Yamamoto S, Masuda S, Yasufuku H, Ueno N, Harada Y, Kato M, Sakai Y. *J. Appl. Phys.* 1997; **82**: 2954.
8. Maus-Friedrichs W, Wehrhahn M, Dieckhoff S, Kempter V. *Surf. Sci.* 1990; **237**: 257.
9. Stracke P. Elektronenspektroskopische Untersuchungen der Metalladsorption auf MgO, Doctoral Thesis, Technische Universität Clausthal, 2000.
10. Lilienkamp G, Koziol C, Schmidt Th, Bauer E. *In X-ray Microscopy and Spectromicroscopy*, Thieme J, Schmahl G, Rudolf D, Umbach E (eds). Springer Verlag: Heidelberg 1998; III.
11. Wei H, Maus-Friedrichs W, Lilienkamp G, Kempter V, Helmbold J, Gömann K, Borchardt GJ. *J. Electroceram.* 2002; **8**: 221.

Surface and Interface Analysis

12. Imbihl R, Ertl G. *Chem. Rev.* 1995; **95**: 697.
13. Gorodetski V, Lauterbach J, Rotermund HH, Block JH, Ertl G. *Nature* 1994; **370**: 277.
14. Sachs C, Hildebrand M, Völkening S, Wintterlin J, Ertl G. *J. Chem. Phys.* 2002; **116**: 5759.
15. Naumovets AG, Zhang ZY. *Surf. Sci.* 2002; **500**: 414.
16. Ichinokawa T, Hamaguchi I, Hibino M, Kirschner J. *Surf. Sci.* 1989; **209**: L144.
17. Marbach H, Günther S, Luerssen B, Gregoratti L, Kiskinova M, Imbihl R. *Catal. Lett.* 2002; **83**: 161.
18. Marbach H, Günther S, Luerssen B, Imbihl R, Gregoratti L, Barinov A, Kiskinova M. *Surf. Rev. Lett.* 2002; **9**: 751.
19. Lilienkamp G, Wei H, Maus-Friedrichs W, Kempter V, Marbach H, Günther S, Suchorski Y. *Surf. Sci.* 2003; **532**: 132.
20. Naumovets AG. In *The Chemical Physics of Solid Surfaces* vol. 7, King DA, Woodruff DP (eds). Elsevier: Amsterdam, 1994; 163.
21. Yakovkin IN, Chernyi VI, Naumovets AG. *Surf. Sci.* 1999; **442**: 81.
22. Losovyj YB, Ketsman IV, Kostrobij P, Suchorski Y. *Vacuum* 2001; **63**: 277.
23. Stultz J, Krischok S, Goodman DW. *Langmuir* 2002; **18**: 2962.

DOI: 10.1002/sia